ELSEVIER
Nuclear Instruments and Methods in Physics Research B 166–167 (2000) 1–12
NIM B
Beam Interactions with Materials & Atoms
www.elsevier.nl/locate/nimb

# Atomistic modelling of radiation effects: Towards dynamics of exciton relaxation

Alexander L. Shluger [a,*], Jacob L. Gavartin [a], Marek A. Szymanski [a,b], A. Marshall Stoneham [a]

[a] *Department of Physics and Astronomy, University College London, Gower Street, London, WC1E 6BT, UK*
[b] *Institute of Physics, Warsaw University of Technology, ul. Koszykowa 75, 00-662 Warsaw, Poland*

**Abstract**

This brief review is focused on recent results of atomistic modelling and simulation of exciton related processes in ionic materials. We present an analysis of thermal fluctuations of the electrostatic potential in cubic ionic crystals and their relation to formation of a tail in the electron density of states and localisation of electronic states. Then the possible 'fast' mechanism of formation of F–H pairs in KBr as a result of decomposition of relaxing excitons is discussed. We briefly describe some ideas related to the possibility of coherent control of exciton decomposition into Frenkel defects in alkali halides. Next we turn to the results of modelling of exciton excitation and localisation at the low-coordinated surface sites of MgO. And finally, we present the results of quantum-mechanical simulation of peroxy linkages and their reaction which creates oxygen molecules in silica. 

*PACS:* 61.70b; 61.80 b + c; 77.84.Bw; 78.40.Ha
*Keywords:* Insulators; Excitons; Surfaces; Radiation defects

## 1. Introduction

Energy and charge localisation are important pre-requisites of material's modification by irradiation [1,2]. Examples include decomposition of localised excitons into defects in alkali halides, alkali-earth fluorides, silica and other materials [3–5], and, more commonly, formation of electron and hole polarons [6]. In this paper, we review some of the recent experimental developments which open new avenues for further understanding of the micro-mechanisms of these phenomena and the related results of our recent theoretical modelling.

Experimental studies and theoretical modelling of excitons and hole polarons have so far been successful mainly in revealing the spectroscopic properties of relaxed states [5,6] rather than the dynamics of rapid localisation process. Although such dynamical effects as hot luminescence of self-trapping excitons (see, for example, [7,8]) and time-resolved relaxation of vibrationally excited

* Corresponding author. Tel.: +44-171-391-1312; fax: +44-171-391 1360.
*E-mail address:* a.shluger@ucl.ac.uk (A.L. Shluger).

0168-583X/00/$ - see front matter 
PII: S0168-583X(99)00734-X

self-trapped excitons (STE) [9] have been demonstrated, the atomistic mechanisms of self-trapping remain unclear. Recent developments of time-resolved spectroscopies allow one to probe the intermediate states of exciton and hole relaxation [8–11]. However, these spectroscopic data cannot be directly related to atomistic models of relaxation processes without further theoretical analysis. The data presented at this meeting by Lushchik [12] demonstrate a much higher yield of formation of stable F centres in KCl as a result of the STE creation by excitation in the region of the Urbach tail than at higher photon energies. These results provide strong impetus for further theoretical studies of precursors for and initial stages of exciton localisation in insulators. Although some ideas regarding the importance of thermal atomic fluctuations for both understanding the nature of the Urbach tail and the formation of precursor states for self-trapping have been suggested in previous studies (see, for example, [13,14]), atomistic models of these states in real systems are missing. To get a deeper insight into the atomic structure of possible precursor states we will present the preliminary results of our modelling of potential fluctuations in MgO, and the mechanism of 'fast' formation of a pair of Frenkel defects in KBr: an F centre (an electron trapped by a halogen vacancy) and an H centre (an interstitial halogen atom in the form of $Br_2^-$ at a single halogen site).

Recent time-resolved laser spectroscopic studies have also demonstrated the coherence of the exciton state in NaCl during several pico-seconds [9]. One of the potential implications of that is the possibility of coherent control of exciton self-trapping and decomposition into defects using specially tailored laser pulses. Coherent control of chemical reactions is a hot topic in molecular reactions in the gas phase [15,16] and some first steps in the direction of coherent control of exciton decomposition in $CaF_2$ have been presented at this meeting by Reichling [17]. We will briefly discuss possible scenarios of coherent control of these processes.

Important applications of radiation effects discussed at this meeting are concerned with low-dimensional systems including one-dimensional crystals, surfaces and nano-particles. However, little is still known about the behaviour of excitons in these systems. We will illustrate the role of low-coordinated surface sites in exciton localisation on the example of low-coordinated surface states of MgO.

Finally, we will turn to a more traditional topic of these meetings related to the mechanisms of radiolysis of insulators. Recent experimental results by the group of Hosono [18] demonstrate that oxygen molecules are one of the main products of the radiolysis of wet amorphous silica due to irradiation by fast protons creating electronic excitations. It is known that electronic excitation of silica leads to formation of localised excitons [19–21] and their decomposition into Frenkel defects [21]. Some 10 years ago using quantum-mechanical modelling of $\beta$-cristabalite [22,23] and $\alpha$-quartz [24] we have proposed a model of a self-trapped exciton and defect pair in these crystals. The latter includes the oxygen vacancy and the peroxy linkage. These results are supported by the recent density functional calculations presented at this meeting by Corrales [25]. In this paper, we demonstrate that the reaction between two peroxy linkages can lead to formation of oxygen molecules and suggest that this is one of the possible mechanisms of formation of these species in irradiated silica.

## 2. Exciton self-trapping and decomposition

The localisation of excitons can be driven in several ways. Clearly, defects or impurities may be able to trap excitons. For example, a very similar dependence of the stable F centre yield in nominally pure KCl as a function of photon energy to that found by Lushchik et al. [12] has been attributed in [26] to the presence of small concentrations of Br ions in these crystals and formation of hetero-nuclear excitons. Similarly, in an amorphous solid, there will be sites of lower energy for excitons. Even if these defects or special sites are unable to trap the exciton, the combination of the inhomogeneity and electron-lattice coupling can often cause trapping. But what happens in a defect-free, impurity-free crystal?

There are fluctuations (of potential and of force-constants) simply from thermal vibrational motion on a time scale similar to that of self-trapping relaxation. So how does localisation occur in these cases? And can we relate it to the so-called Urbach tail, which describes the band edge in many solids by a characteristic energy dependence. Like self-trapping, the Urbach edge involves some combination of static fluctuations (e.g., due to impurities), dynamic fluctuations, and electron-lattice coupling.

### 2.1. Analysis of atomic fluctuations

The role of dynamic potential fluctuations in formation of Urbach tail in optical absorption of insulators and semiconductors, and in exciton and polaron self-trapping has been considered previously (see, for example, [13,14,27,28]). However, atomistic models which would allow one to link these fluctuations with the quantum-mechanical modelling of excitons using conventional many-electron methods are still missing. Recent modelling of the electron and phonon localisation in amorphous silicon and in silica glass [29–31] has demonstrated that numerical approaches can provide useful insight into the atomic nature of localised states (LS) induced by static disorder. In this paper, we present the results of our modelling of potential fluctuations and localisation of electronic states due to dynamical thermal disorder. To be specific, we have chosen a cubic oxide MgO which can be well described using semi-empirical classical and quantum-mechanical atomistic simulation methods.

First, we performed the shell model (NVE) molecular dynamics (MD) simulations in order to study the classical evolution of the system of 512 ions at different temperatures using the interatomic potentials [32] and the GULP code [33]. From the obtained MD trajectories several non-correlated instantaneous configurations were chosen whose potential energy is close to its mean value. These static configurations represent the class of most probable configurations occurring in our classical dynamical system. Thus generated configurations were then used to calculate the one electron spectra and the on-site electrostatic potentials within the semi-empirical Hartree–Fock (HF) method in the INDO approximation [34]. Comparison of the classical shell model and the INDO calculations for the same configurations has demonstrated very similar (within 0.1 eV) relative energies of different configurations. The probability distributions of electrostatic potentials calculated on system ions by both methods are also very similar, which confirms their compatibility. The one electron spectra calculated in the INDO approximation for different configurations have been used to analyse the effect of thermal disorder on the density of states (DOS) and localisation of the electronic states. The system was characterised by fluctuations of on-site electrostatic potentials and ionic charges and degree of localisation of electronic states. These have been calculated in the following way.

In the INDO method the one-electron wavefunctions are calculated as a linear combination of atomic orbitals (AO) (in the case of MgO, we consider valence s-orbitals on magnesium ions and s- and p-valence orbitals on oxygen ions)

$$\psi(E) = \sum_{i\alpha_i} C_{i\alpha_i}(E)\phi\alpha_i.$$

Here $i$ numerates the atoms and $\alpha_i$ numerates the AO on the atom $i$, $C_{i\alpha_i}(E)$ is the coefficient of the AO $\alpha_i$ in the LCAO expansion for the eigen-state with the energy $E$. Using this representation, the degree of localisation of each electron state can be characterised using, for example, the inverse participation function [35] $p(E)$, or energy dependent localisation length [36] $\xi(E)$. Both parameters give an indication of over how many atoms the state in question is spread. The latter parameter has an advantage of containing an additional information of how far apart the localisation centres are. In case of truly extended one-electron states $p(E)$ takes the value of the number of atoms in the sublattice, while $\xi(E)$ takes the value of the giro radius of the system $R_g$. For the periodic system with a closest image convention, $R_g$ is a half of a linear size of the system, which is equal to four in our case.

In order to study the correlation between the localisation and electrostatic potential and charge

fluctuations we exploit the same idea and introduce the energy dependent electrostatic potential fluctuation $\Delta U(E)$,

$$\Delta U(E) = \sum_{i\alpha_i} C^2_{i\alpha_i}(E)(U_i - \langle U\rangle),$$

and the energy dependent ionic charge fluctuation $\Delta Q(E)$,

$$\Delta Q(E) = \sum_{i\alpha_i} C^2_{i\alpha_i}(E)(Q_i - \langle Q\rangle).$$

These two parameters significantly deviate from zero only for those states where the localisation and potential (charge) fluctuation of the particular sign occur on the same ions.

A schematic diagram illustrating deviations of the instantaneous on-site electrostatic potentials $U_m$ (dashed lines) from their perfect lattice values (solid line), due to thermal ionic disorder is shown in Fig. 1. These deviations give rise to a finite width of probability distributions for the potential fluctuations on the cation and anion sites. Such distributions are depicted in the lower left part of the diagram where $\langle U_{Mg}\rangle$ and $\langle U_O\rangle$ are the mean values of potentials at the cation and anion site, respectively. Note that these distributions are not necessarily Gaussian and can be different for different sub-lattices. Particular potential fluctuations, namely those from the lower amplitude distribution tails, are causing the appearance of the tails of the electronic DOS at the top of the valence band (potential fluctuations in the anion sub-lattice) and at the bottom of the conduction band (potential fluctuations in the cation sub-lattice). These fluctuations are shown as the corresponding shaded areas at the potential distributions. The correlation between fluctuations of the electrostatic potential, $\Delta U(E)$, the correlation length of electronic states, $\xi(E)$, and the electronic DOS is demonstrated in Fig. 2. The

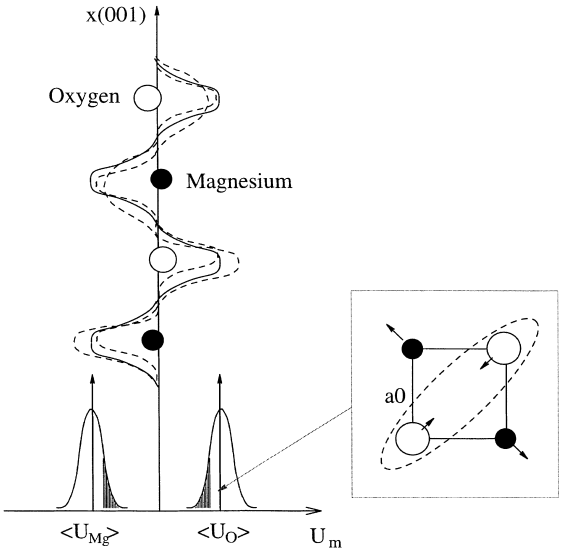


Fig. 1. Schematic diagram illustrating deviations of the instantaneous on-site electrostatic potentials $U_m$ (dashed lines) from their perfect lattice values (solid line) due to thermal disorder. Such deviations give rise to a finite width of probability distributions of the potential fluctuations on the cation and anion sites shown in the lower left part of the diagram. The critical fluctuations from the shaded tail of the anion distribution are statistically more likely to appear on the neighbouring anion sites. A statistically most probable atomic model of such fluctuations on anion sites is depicted in the inset on the right.

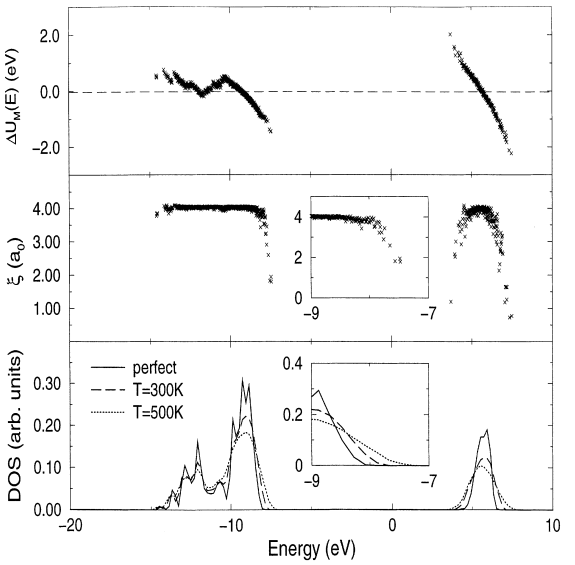


Fig. 2. The electron density of states (lower plot), the energy dependent correlation length (medium plot), and the energy dependent electrostatic potential fluctuation (top plot) of the MgO crystal. The insets represent the enlarged area of the top of the valence band tail. The temperature effect on the tails of the DOS is shown in the lower plot, where the DOS for 300 K (dashed line) and 500 K (dotted line) are compared with the DOS for the perfect lattice. The energy dependent correlation length and potential fluctuations are shown only for 500 K.

atomic configurations were generated by the molecular dynamics simulations at temperatures 300 and 500 K.

One can see that the electrostatic potential fluctuations are the strongest at the energies corresponding to the top of the valence band and the bottom of the conduction band, where the correlation length of electronic states strongly deviates from four, which is the half of the periodic cell length and corresponds to the completely delocalised states. This deviation corresponds to localisation of electronic states (which is strongest in the tail) and their splitting from the delocalised states and formation of a tail in the DOS. The blown up figures of tails in the correlation length and DOS are shown in insets in Fig. 2, the DOS corresponding to the perfect lattice is shown by a solid line for comparison. One can see the strong dependence of the tail in the DOS on temperature, known from previous works. Comparing these data with the energy dependent ionic charge fluctuations $\Delta Q(E)$ we found that the localised states (LS) from the tail at the top of the valence band are characterised by a persistent positive deviation (of the order of 0.02 $e$, $e$ is the electron charge) of effective charges on the ions where these states are localised, i.e., these are effectively 'hole' states. On the other hand, the ions on which the electronic states corresponding to the tail at the bottom of the conduction band are localised, are more 'negative'.

Having established the link between fluctuations of the electrostatic potential and localisation of electronic states, we can study the spatial aspects and atomic structure of these fluctuations. The first question is whether the potential fluctuations are spatially correlated? Let us define the fluctuation as an event when the on-site electrostatic potential on some ion deviates from its mean value by more than some critical value $U_c$. We shall call this fluctuation isolated, if no similar fluctuation occurred at the same time on any of the nearest neighbour sites of the same species. Assuming a random distribution, the probability to find an isolated fluctuation $p_{isol}$, is related to the probability of finding any fluctuation (isolated or not) $p_{fl}$ as

$$p_{isol}(s) = p_{fl}(s) \times (1 - p_{fl}(s))^z. \quad (1)$$

Here $s$ indicates the anion or cation sub-lattice, and $z$ is the number of the nearest neighbours in the sub-lattice (in MgO $z = 12$). Our analysis of the thermally distorted configurations demonstrates that the number of the isolated fluctuations is 2–5 times (dependent on a choice of a critical threshold, $U_c$) less then that predicted by Eq. (1). This applies to both fluctuations in anion and cation sub-lattices. Therefore we can conclude that fluctuations are likely to occur on the neighbouring sites than on the individual sites. Similarly we have studied the probability for fluctuations in different sub-lattices to occur on the nearest neighbouring sites and concluded that the fluctuations corresponding to the LS in the tail of the valence band and to those in the conduction band are unlikely to occur on the nearest neighbouring sites.

Analysis of the radial distribution function for potential fluctuations from the shaded tail of the anion distribution in Fig. 1 and occurring on two neighbouring sites demonstrates that the nearest cations are more likely to be displaced outwards by about 0.03 $a_0$ ($a_0$ is the lattice constant) with respect to their ideal lattice sites, as schematically depicted by arrows in Fig. 1. Although a similar analysis demonstrates that the two anions involved into the potential fluctuation are likely to be displaced towards each other, our statistics in this case demonstrates a much smaller deviation of the maximum of the radial distribution function from the perfect lattice positions.

To conclude, the analysis of dynamical fluctuations of atoms in a binary cubic ionic system demonstrates the strong correlation between fluctuations from the tails of the electrostatic potential distribution, tail formation in the electronic DOS and localisation of electronic states. These potential fluctuations in one sub-lattice tend to appear on neighbouring ions. Although the modelling has been performed for MgO, we believe that our conclusions are also valid for alkali halides, which have the same crystal structure. It is tempting to directly relate the atomic fluctuations, such as those shown in Fig. 1, to precursors for self-trapping of excitons and holes in these systems. However, our results still do not provide direct evidence for that. We are

currently working on modelling of exciton and hole dynamics in the presence of thermal atomic fluctuations.

Experimentally, there have been several recent studies of the dynamics of spectroscopic changes in the energy range of 1.5–3.2 eV in alkali halides during the hole self-trapping [37,38]. Although very stimulating, they proved to be inconclusive as the time-resolved spectra have been contaminated by the two-photon cross-correlation of the excitation and probe beams [11]. Therefore the issue of precursors for self-trapping and dynamics of self-trapping process in these systems is still unresolved. It is complicated by the presence of random strains and static random electric fields of order $10^5$ V/cm in real samples [39].

### 2.2. Fast mechanism of F centre formation in KBr

Some additional clues regarding the dynamics of exciton relaxation can be obtained by monitoring the time-evolution of creation of Frenkel defects in alkali halides. It has recently been shown that in KBr and RbBr the generation of a Frenkel pair consisting of an F centre and an H centre takes place through two different processes: the fast process which terminates within a few ps after the excitation, and the slow process which continues after the fast process has terminated for over 100 ps at low temperature [40]. The mechanism of the fast process, which plays a central role in formation of the F–H pairs at low temperatures, remains unclear.

The two-photon excitation with an energy of about 8 eV employed in these experiments produces electron-hole pairs in the bulk of the crystals. The electron is shown to be initially delocalised in the lattice [41], whereas the hole localises and after relaxation becomes a $V_K$ centre ($Br_2^-$ molecular ion situated in two lattice sites) [5]. One of the characteristic features of the fast process is that it takes place before the relaxation of the holes into their most stable configuration, the $V_K$ centre, is completed [40]. Therefore it has been suggested that the fast process of the F–H pair formation is due to the interaction of the electrons with relaxing holes [40].

This model has been analysed in our recent work [42] using the ab initio HF calculations which self-consistently account for lattice polarisation. The starting hole configuration has been chosen close to that shown in Fig. 1. The two-centre model of the initial localised hole state assumes that the hole is shared by the two nearest neighbour Br ions situated close to their lattice sites. It has been found that if the distance, $R$, between the two Br ions carrying the hole is larger than a critical value $R_c$ of about 3.65 Å, the energy of the two-centre hole state is higher than that of the 'one-centre' relaxed state. The latter corresponds to a preferable localisation of the hole on one Br ion with a adiabatically adjusted lattice relaxation. The value of $R_c$ is by about 0.55 Å longer than the equilibrium distance in the $V_K$ centre. Therefore, at the Br–Br distances longer than $R_c$, any asymmetric lattice distortion polarises the system towards the one-centre hole state. This results from the interplay between the lattice polarisation which favours the charge localisation, and the chemical bonding between the $Br^0$ and the surrounding Br ions, which is weak at long distances, as discussed in [43]. The resulting adiabatic potential of the hole transformation into the two-centre state along $R$ is very soft. Analysis of the forces acting on ions during the relaxation of the system when an electron is trapped by the relaxing hole shows that they drive the downhill relaxation and formation of the separated F–H pair because the initial hole configuration is already favourable for this process. The large excess energy leads to a high probability to overcome the separation barrier. Therefore it has been concluded that the fast process of the F–H pair formation in KBr prior to the hole self-trapping is driven by the interaction of the relaxing hole with the electron, and a significant part of the exciton relaxation energy is imparted into the displacement mode of the halogen molecular ion along the $\langle 1\,1\,0\rangle$ axis. Like the results by Lushchik et al. [12], these data suggest that the formation of stable separated defect pairs happens during relaxation in the ground electronic state of triplet excitons.

### 2.3. Coherent control

The results presented above demonstrate considerable progress in understanding the mechanisms and dynamics of photo-induced processes in ionic solids, in particular hole and exciton self-trapping. Recent experimental developments in ultrafast optical techniques in producing waveforms with specified time-dependent amplitude, phase, frequency and polarisation [44] open, however, new opportunities. The focus of ultrafast spectroscopies is now shifting from observation into applications of light, exploiting specially designed profiles of the above parameters so as to guide the quantum dynamics of a system to a particular target. It has indeed been demonstrated that tailoring of light fields and their interference can be used to *control* wavepacket dynamics and chemical reactions in the gas phase, such as system propagation along a single vibration mode or reaction along a single chemical pathway (see recent reviews [15,16]). The theory of active control of molecular motion by the use of shaped laser pulses has been developing for several years (see, for example, [45–47]). There have been applications of this theory to dissipative systems [48,49], but no systematic analysis of the possibilities of quantum control in crystals. Why it can be useful? If successful, it can provide smart ways how to control, for example, defect luminescence yields and yields of defect production under laser excitation in the bulk, and laser-induced desorption and dissociation of molecules at surfaces. However, the main problem is fast loss of coherence: defects in crystal are not vibrating 'in step' due to strong interaction with crystal phonons.

A class of photo-induced reactions in polar solids, where quantum control seems realistic, is self-trapping of excitons and their decomposition into Frenkel defects. The feasibility of this idea is supported by the experimental results of Tanimura's group [9] which demonstrated that the dissipation and dephasing of a vibrationally excited STE state in NaCl occurs during several ps, preserving coherent oscillations of the system between two states. Tanimura and Itoh [50] have found that sequential excitation of STE with pulses having chosen wavelength and polarisation can affect the exciton relaxation and defect production. This suggests that one can try the so-called 'pump–dump' scenario [16] of quantum control of the exciton decomposition and the defect yield. This involves exciting a relaxed STE into the dissociative electronically excited state by the first femtosecond pulse, and then dumping a wave-packet into one of the nearest F–H pair states by applying the second pulse causing stimulated emission. This requires careful calculation of the photon energy of the dump pulse and timing between pulses. If successful, one could avoid losses due to exciton luminescence and non-radiative transition into the crystal ground state. Another scenario could involve special tailoring of the form of exciton excitation pulse that to facilitate the 'fast' mechanism of defect production in the ground state of STE. We are currently exploring these possibilities theoretically in collaboration with experiment.

## 3. Excitons at low-coordinated surface sites of MgO

Interaction of radiation with real surfaces, powders, nano-particles, quantum dots and other systems, where reduced dimensions or atomic coordination can play significant role, is a growing area of research. Photons can create excitons, produce ablation, trigger surface reactions and desorption of molecules. However, the absorption and luminescence energies and behaviour of excited states at surfaces can be very different from those in the bulk. To demonstrate this point we turn once again to MgO where excitons do not self-trap in the bulk but can localise at low-coordinated surface sites.

The reduced ion coordination in ionic oxides, such as MgO materials leads to significant changes in the crystalline potential [51] which have been correlated with the chemical (see, for example, recent discussion [52]) and spectroscopic [51,53] properties of the low-coordinated surface sites. Experimentally, several spectroscopic features have been attributed to the presence of these sites. In particular, the High Resolution Electron Energy Loss Spectra of MgO have demonstrated that the exciton absorption peak shifts from 7.7 eV in the bulk [54] to 6.15 eV at the (0 0 1) surface plane

[55]. The ultra-violet diffuse reflectance spectra of micro-crystalline MgO have demonstrated additional bands at 5.7 and 4.6 eV, which have been attributed to the low-coordinated sites, such as steps, kinks and corners [53,56]. Coluccia et al. [57–59] have studied the photo-luminescence of powdered MgO excited in these bands and have observed broad luminescence spectra. Both the excitation and emission spectra demonstrate a strong dependence on the powder preparation and treatment with different gases [58,59]. They were attributed to the excitation and luminescence of excitons at different low-coordinated sites at powder surfaces. Very similar features have been observed in the excitation and emission spectra of the other cubic oxides CaO, SrO, BaO [56–60]. The proposed interpretations of the spectroscopic data imply a dramatic dependence of the spectroscopic properties of oxide surfaces on the ion coordination. In particular, the exciton excitation energy is thought to be reduced from 7.7 eV in the bulk to about 4.6 eV at the three-coordinated sites. However, direct experimental verification of these models is presently very difficult.

Our recent calculations [61] have confirmed the strong dependence of spectroscopic properties on coordination, and the possibility of selective optical excitation of low-coordinated surface sites. This results from a combination of several interrelated factors which include the reduction of the Madelung potential at low-coordinated sites leading to their substantial relaxation with respect to ideal geometry and to strong electron density redistribution. Our results have demonstrated the consistent reduction of the excitation energies with decrease of coordination of surface sites and qualitatively supported the assignment of the peaks at about 5.7 and 4.6 eV to the four- and three-coordinated oxygen surface sites, respectively [53]. The excited states appear to be more localised at the terminating three-coordinated oxygen sites, than within the edge or at the surface. The relative energies of the excited states corresponding to oxygen sites of different coordination suggest the possibility of the excitation transfer from, e.g., the surface to the more localised terminating corner sites with lower energy. Similar behaviour of the excitation was proposed in [57] on the basis of analysis of the experimental data, however, the mechanism of this process requires more detailed study.

## 4. Mechanism of formation of $O_2$ in irradiated silica

Silicon dioxide is another material where radiation effects are largely governed by the exciton localisation, which happens in both $\alpha$-quartz and amorphous material. However, the exciton decomposition into Frenkel defects is effective only in amorphous silica and its details are still unknown. We show that recent calculations can give a coherent picture of the defect creation process in silica, if we assume that exciton decomposition leads to formation of neutral oxygen vacancies and peroxy linkages.

Recent experiments by Hosono et al. [18] provided some evidence for Frenkel defect formation in wet synthetic silica glass irradiated by 10 MeV protons. They demonstrated the formation of neutral and positively charged oxygen vacancies (Si–Si bonds and E' centres), and of interstitial oxygen molecules and peroxy radicals in comparable concentrations. However, the mechanism of formation of $O_2$ molecules is unclear. Tsai and Griscom [62] proposed that they can be created through the biexciton process as a result of dense electronic excitation. The model calculations [23] for $\beta$-cristobalite suggested the STE decomposition into oxygen vacancy and "peroxy bridge" pair. However, the electronic structure of this pair has not been clearly established. If we assume that a neutral vacancy and a peroxy linkage (a form of incorporation of oxygen atom into the silica network) is formed, then perhaps the reaction between two peroxy linkages (PLs) can lead to production of $O_2$ molecules. In order to check this idea, we have modelled the properties of PLs and their reaction in $\alpha$-quartz.

The calculations were performed using the density functional theory (DFT) based method in the basis of plane waves, using the Perdew–Wang functional and the generalised gradient approximation (GGA) [63,64]. The "ultrasoft" pseudopotentials implemented in the VASP code [65,66] allow us to use a relatively small plane wave cut-off

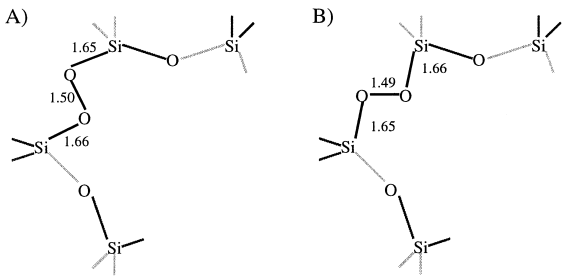


Fig. 3. Schematic of two stable configurations of the peroxy linkage in α-quartz. Numbers show the bondlength in Ångstroms.

of 400 eV. The periodic cell included 72 ions and the calculations were performed in the $\Gamma$ point of the Brillouin zone. For charged defects, a monopole–monopole correction introduced by Makov and Payne [67] was employed.

Two stable configurations of the PL defect are shown in Fig. 3. They can be viewed as the same Si–O–O–Si complex rotated around the line connecting two nearest Si ions and are different due to a small inequivalency of pairs of Si–O bonds in α-quartz. The energy difference between the two configurations is 0.18 eV. The barrier for rotation of the – O–O – complex from the lower energy configuration B into the higher energy configuration A is 0.57 eV. The calculated formation energy of a separated PL and a neutral oxygen vacancy defect is 7.39 eV, which is lower than the exciton excitation energy. The DFT method allows us to calculate only the singlet-triplet excitation energy of PL, which was found to be equal 4.1 eV.

Ionisation of PL leads to the formation of a well known paramagnetic peroxy radical defect and shortening of the O–O bond in the Si–O–O–Si bridge to 1.38 Å. This configuration was found to

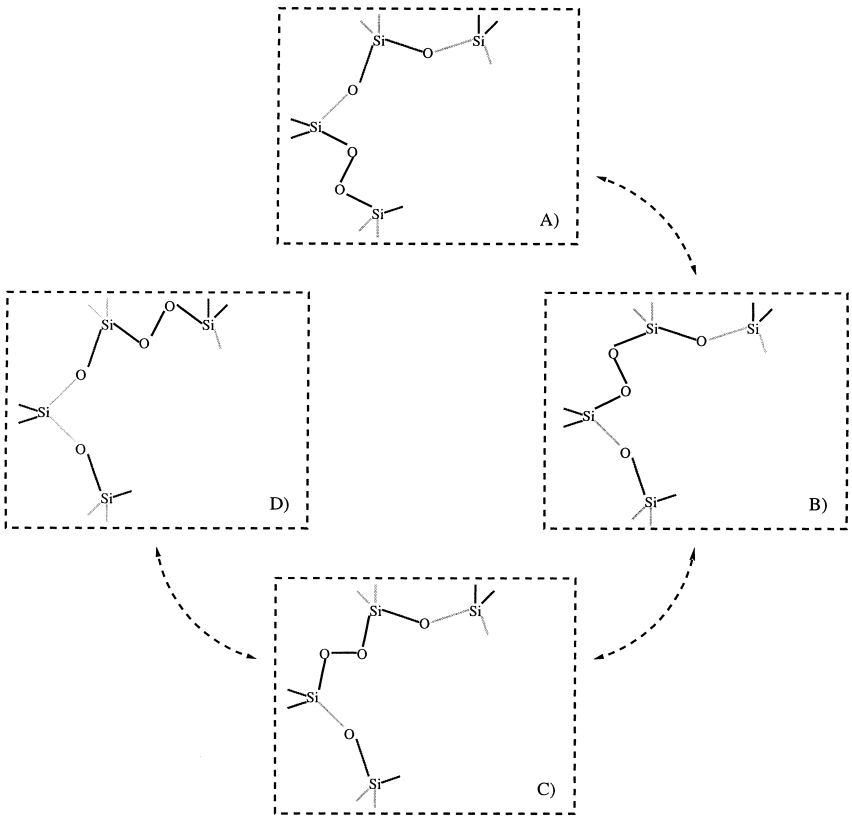


Fig. 4. Schematic presentation of the four stages of the peroxy linkage diffusion along the *c*-axis in α-quartz.

have about 0.7 eV lower energy in α-quartz than another, more conventional, Si–O–O configuration. The electron affinity of the relaxed peroxy radical to an electron from the conduction band was found to be about 8.8 eV. Some other ways to produce a peroxy linkage include the direct incorporation of an oxygen atom into a regular Si–O–Si bond, or a recombination of either a neutral oxygen molecule with a neutral oxygen vacancy, or of a negatively charged oxygen molecule with a positively charged E' centre. Both latter reactions are exothermic.

Diffusion of peroxy linkages differs in different channels of the α-quartz structure. The easiest diffusion is along the *c*-axis, and its stages are shown schematically in Fig. 4. The diffusion mechanism involves transfer of an oxygen atom between the two equivalent peroxy configurations as shown in Fig. 5, and rotation of PL between the low and high energy configurations. The energy surface for diffusion is also shown schematically in Fig. 5. The highest energy barrier for diffusion is about 1.3 eV, which is similar to that predicted by Hamann [68].

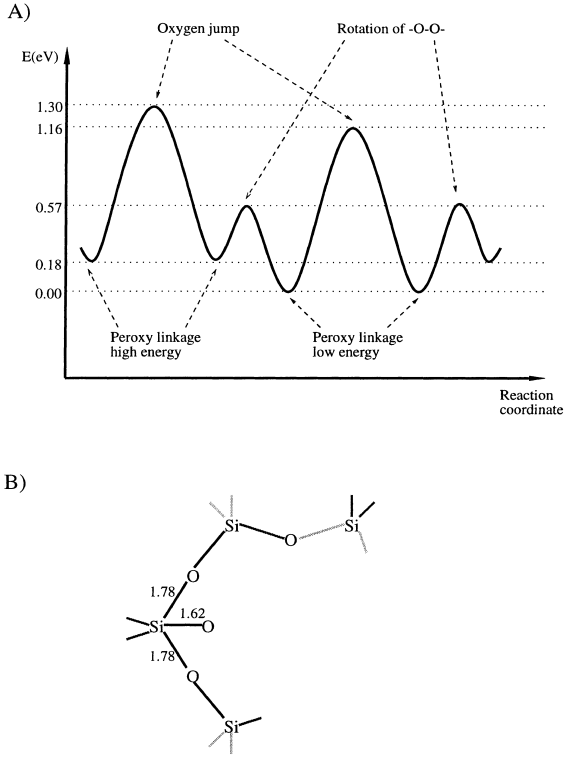


Fig. 5. Schematic diagram of the adiabatic potential for the peroxy linkage diffusion along the *c*-axis in α-quartz, and the typical transition state showing the bondlengths in Ångstroms.

The reaction between the two peroxy linkages is shown in Fig. 6. When the two defects occur in the two neighbouring sites, as shown in the inset D, the system can transform through the barrier configuration C into the state A where the oxygen molecule is in the interstitial position. The initial transformation is driven by a translation of one of the oxygen atoms ($O_2$ in Fig. 6(C)) almost like in the diffusion process. However, the barrier is lowered by the formation of a chemical bond between $O_1$ and $O_2$ (Fig. 6(B)) and spin flipping from the initial singlet state into the triplet state localised on the oxygen molecule. The barrier for this solid state reaction was found to be equal about 1.0 eV, whereas the energy gain is about 2.3 eV. The latter depends on the initial configuration of the two peroxy linkages.

These calculations present an example of the possibilities of computer modelling in studying some complex radiation induced processes in solids. Another example has been provided at this meeting by the group of Corrales who presented the results of their recent calculations of the self-trapped exciton and some defect centres in α-quartz.

## 5. Futures

We hope that this brief review presents an encouraging example of collaboration between experiment and theory and demonstrates some of the possible directions into the future research of the mechanisms of radiation-induced effects in ionic materials. We have not touched on the area of organic and one-dimensional materials. Zero-point energies can be important for more accurate understanding of the behaviour and thermal fluctuations of even semi-classical systems. How to handle non-adiabatic cases and dissipation both in the electronic and vibrational motion remain among the most pressing problems of modelling of radiation damage.

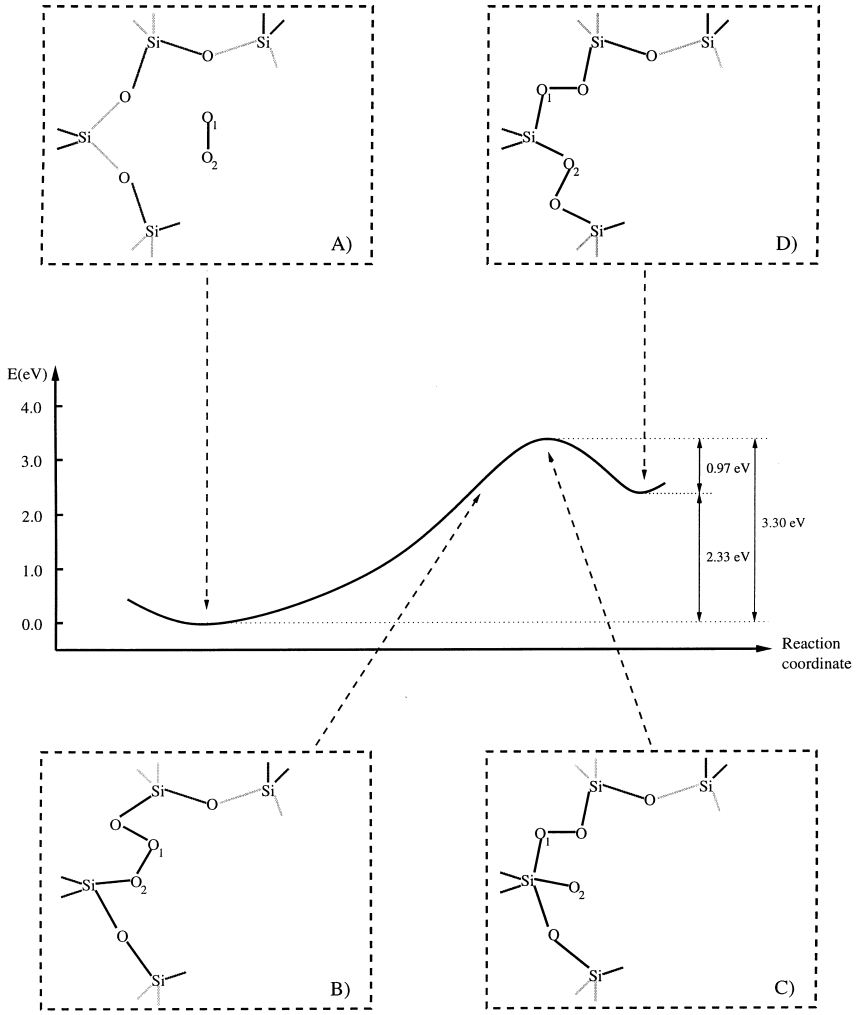


Fig. 6. Schematic diagram of the reaction between two peroxy linkages (D) with formation of the oxygen molecule in the interstitial (A), showing two intermediate configurations (B) and (C) and their relative energies. The adiabatic curve in the middle has only illustrative meaning.

## Acknowledgements

JLG would like to thank the Leverhulme Trust for financial support. MS is grateful to FECIT for financial support. We are grateful to K. Tanimura, R.T. Williams, A. Lushchik, M. Reichling, L. Kantorovich, P. Sushko, P. Saalfrank and R. Corrales for valuable discussions, and to A. Lushchik, M. Reichling and R. Corrales for details of their work prior to publication.

## References

[1] A.M. Stoneham, Nucl. Instr. and Meth. Phys. Res. A 91 (1994) 1.
[2] A.M. Stoneham, Rad. Eff. Def. Solids 142 (1997) 191.
[3] Ch.B. Lushchik, A.Ch. Lushchik, Decay of Electronic Excitations with Defect Formation in Solids, Nauka, Moscow, 1989.
[4] N. Itoh (Ed.), Defect Processes Induced by Electronic Excitation of Insulators, World Scientific, Singapore, 1989.
[5] K.S. Song, R.T. Williams, Self-Trapped Excitons, Springer, Berlin, 1993.

[6] A.L. Shluger, A.M. Stoneham, J. Phys.: Condens. Matter 5 (1993) 3049.
[7] V.V. Hizhnyakov, V.G. Plekhanov, V.V. Shepelev, G.S. Zavt, Phys. Stat. Sol. (b) 108 (1981) 531.
[8] S. Tomimoto, H. Nansei, S. Saito, T. Suemoto, J. Takeda, S. Kurita, J. Lumines. 76&77 (1998) 491.
[9] T. Makimura, K. Tanimura, N. Itoh, T. Tokizaki, A. Nakamura, J. Phys.: Condens. Matter 5 (1994) 4581.
[10] H. Fujiwara, T. Suzuki, K. Tanimura, J. Phys.: Condens. Matter 9 (1997) 923.
[11] E.D. Thoma, H.M. Yochum, R.T. Williams, Phys. Rev. B 56 (1997) 8001.
[12] A. Lushchik, M. Kirm, Ch. Lushchik, E. Vasil'chenko, Nucl. Instr. and Meth. B 166–167 (2000) 529.
[13] H. Sumi, Y. Toyozawa, J. Phys. Soc. Jap. 31 (1971) 342.
[14] M. Ueta, H. Kanzaki, K. Kobayashi, Y. Toyozawa, E. Hanamura (Eds.), Exciton Processes in Solids, Springer, Berlin, 1986.
[15] M. Shapiro, P. Brumer, J. Chem. Soc. Faraday Trans. 93 (1997) 1263.
[16] R.J. Gordon, S.A. Rice, Annu. Rev. Phys. Chem. 48 (1997) 601.
[17] R. Lindner, M. Reichling, Paper at this meeting.
[18] H. Hosono, H. Kawazoe, N. Matsunami, Phys. Rev. Lett. 80 (1998) 317.
[19] A.N. Trukhin, A.E. Plaudis, Fiz. Tverd. Tela (Leningrad) 21, (1979) p. 1109.
[20] A.N. Trukhin, Phys. Stat. Sol. B 98 (1980) 541.
[21] D.L. Griscom, in: Proceedings of the 33rd Frequency Control Symposium, Electronic Industries Association, Washington, DC, 1979.
[22] A.L. Shluger, J. Phys. C: Solid State Phys. 21 (1988) L431.
[23] A.L. Shluger, E.V. Stefanovich, Phys. Rev. B 42 (1990) 9664.
[24] A.J. Fisher, W. Hayes, A.M. Stoneham, Phys. Rev. Lett. 64 (1990) 2667.
[25] J. Song, H. Jónsson, L.R. Corrales, Nucl. Instr. and Meth. B 166–167 (2000) 451.
[26] M. Maki, N. Nagasawa, M. Hirai, in: Proceedings of International Conference on Color Centers in Ionic Crystals, Sendai, 1974.
[27] V. Sa-yakanit, H.R. Glyde, Comments Cond. Mat. Phys. 13 (1987) 35.
[28] P. van Mieghem, Rev. Mod. Phys. 64 (1992) 755.
[29] F. Finkemeier, W. von Niessen, Phys. Rev. B 58 (1998) 4473.
[30] M.-Z. Huang, L. Ouyang, Q.Y. Ching, Phys. Rev. B 59 (1999) 3540.
[31] S.N. Taraskin, S.R. Elliott, Phys. Rev. B 59 (1999) 8572.
[32] A.L. Shluger, A.L. Rohl, D.H. Gay, R.T. Williams, J. Phys.: Condens. Matter 6 (1994) 1825.
[33] J.D. Gale, J. Chem. Soc. Faraday Trans. 93 (1997) 69.
[34] E.V. Stefanovich, E.K. Shidlovskaya, A.L. Shluger, M.A. Zakharov, Phys. Stat. Solid (b) 160 (1990) 529.
[35] R.J. Bell, Discuss. Faraday Soc. 50 (1970) 110.
[36] D.E. Sigeti, X. Zhang, M.S. Friedrich, R.A. Friesner, Phys. Rev. B 44 (1991) 614.
[37] S. Iwai, T. Tokizaki, A. Nakamura, K. Tanimura, N. Itoh, A. Shluger, Phys. Rev. Lett. 76 (1996) 1691.
[38] H. Fujiwara, T. Suzuki, K. Tanimura, Mater. Sci. Forum 239–241 (1997) 561.
[39] A.M. Stoneham, Rev. Mod. Phys. 41 (1969) 82.
[40] T. Sugiyama, H. Fujiwara, T. Suzuki, K. Tanimura, Phys. Rev. B 54 (1996) 15109.
[41] G. Petite, P. Daguzan, S. Guizard, P. Martin, Mater. Sci. Forum 239–241 (1997) 555.
[42] A.L. Shluger, K. Tanimura, J. Luminescence 76&77 (1998) 591.
[43] A.L. Shluger, J.D. Gale, Phys. Rev. B 54 (1996) 962.
[44] H. Kawashima, M.M. Wefers, K.A. Nelson, Annu. Rev. Phys. Chem. 46 (1995) 627.
[45] R. Kosloff, S.A. Rice, P. Gaspard, S. Tersigni, D.J. Tannor, Chem. Phys. 139 (1989) 201.
[46] C.J. Bardeen, J. Che, K.R. Wilson, V.V. Yakovlev, V.A. Apkarian, C.C. Martens, R. Zadoyan, B. Kohler, M. Messina, J. Chem. Phys. 106 (1997) 8486.
[47] K. Sundermann, R. de Vivie-Riedle, J. Chem. Phys. 110 (1999) 1896.
[48] J. Cao, M. Messina, K.R. Wilson, J. Chem. Phys. 106 (1997) 5239.
[49] P. Saalfrank, R. Kosloff, J. Chem. Phys. 105 (1996) 2441.
[50] K. Tanimura, N. Itoh, J. Phys. Chem. Solids 45 (1984) 323.
[51] J.D. Levine, P. Mark, Phys. Rev. 144 (1966) 751.
[52] E.V. Stefanovich, T.N. Truong, J. Chem. Phys. 102 (1995) 5071.
[53] E. Garrone, A. Zecchina, F.S. Stone, Phil. Mag. B 42 (1980) 683.
[54] D.M. Roessler, W.C. Walker, Phys. Rev. 159 (1959) 733.
[55] P.A. Cox, A.A. Williams, Surface Sci. 175 (1986) L782.
[56] A. Zecchina, M.G. Lofthouse, F.S. Stone, J. Chem. Soc. Faraday Trans. I 71 (1975) 1476.
[57] S. Coluccia, A.M. Deane, A. Tench, J. Chem. Soc. Faraday Trans. I 74 (1978) 2913.
[58] S. Coluccia, A.J. Tench, R.L. Segall, J. Chem. Soc. Faraday Trans. I 75 (1979) 1769.
[59] S. Coluccia, A. Barton, A.J. Tench, J. Chem. Soc. Faraday Trans. I 77 (1981) 2203.
[60] S. Coluccia, L. Marchese, in: Active Sites and Reaction Mechanisms on the Surface of Basic Catalysts: Spectroscopic Studies, Sapporo, Kodansha, Tokyo, Japan, 1988.
[61] A.L. Shluger, P.V. Sushko, L.N. Kantorovich, Phys. Rev. B 59 (1999) 2417.
[62] T.E. Tsai, D.L. Griscom, Phys. Rev. Lett. 67 (1991) 2517.
[63] J.P. Perdew, in: P. Ziesche, H. Eschrig (Eds.), Electronic Structure in Solids' 91, Academie Verlag, Berlin, 1991.
[64] J.P. Perdew, J.A. Chevary, S.H. Vosko, K.A. Jackson, M.R. Pederson, D.J. Singh, C. Fiolhais, Phys. Rev. B 46 (1992) 6671.
[65] G. Kresse, J. Furthmuller, Phys. Rev. B 54 (1996) 11169.
[66] G. Kresse, J. Furthmuller, Comput. Mater. Sci. 6 (1996) 15.
[67] V. Makov, M.C. Payne, Phys. Rev. B 51 (1995) 4014.
[68] D.R. Hamann, Phys. Rev. Lett. 81 (1998) 3447.